

Submitted by  
**Julian Hofer, B.Sc.**

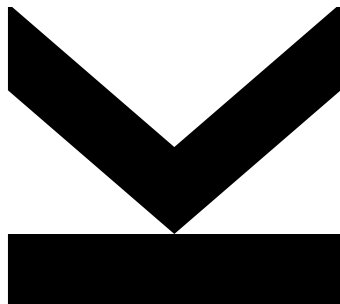
Submitted at  
**Institute of Semicon-**  
**ductor and Solid State**  
**Physics**

Supervisor  
**Prof. Dr. Armando**  
**Rastelli**

Co-Supervisor  
**DI Christian Schimpf**

month year

# Exciting and Resolving Quantum Dot Emission with Adiabatic Rapid Passage and Fabry Perot Interferometer



Master Thesis  
to obtain the academic degree of  
Diplom-Ingenieur  
in the Master's Program  
Technische Physik



---

## Eidesstattliche Erklärung

Ich erkläre an Eides statt, dass ich die vorliegende Masterarbeit selbstständig und ohne fremde Hilfe verfasst, andere als die angegebenen Quellen und Hilfsmittel nicht benutzt bzw. die wörtlich oder sinngemäß entnommenen Stellen als solche kenntlich gemacht habe. Die vorliegende Masterarbeit ist mit dem elektronisch übermittelten Textdokument identisch.

---

Datum

---

Unterschrift



# Acknowledgement

Hello, here is some text without a meaning. This text should show what a printed text will look like at this place. If you read this text, you will get no information. Really? Is there no information? Is there a difference between this text and some nonsense like “Huardest gefburn”? Kjift – not at all! A blind text like this gives you information about the selected font, how the letters are written and an impression of the look. This text should contain all letters of the alphabet and it should be written in of the original language. There is no need for special contents, but the length of words should match the language.

This document is set in Palatino, compiled with pdfL<sup>A</sup>T<sub>E</sub>X2<sub>ε</sub> and Biber.

The L<sup>A</sup>T<sub>E</sub>X template from Karl Voit is based on KOMA script and can be found online:

<https://github.com/novoid/LaTeX-KOMA-template>



# Abstract

This is a placeholder for the abstract. It summarizes the whole thesis to give a very short overview. Usually, this the abstract is written when the whole thesis text is finished.





# Contents

## Abstract

<b>1</b>	<b>Introduction</b>	<b>1</b>
<b>2</b>	<b>Quantum Dot</b>	<b>3</b>
2.1	Processing . . . . .	3
2.2	Properties of our dots . . . . .	3
2.2.1	Calculate spectral range of zero-phonon line . . . . .	3
2.3	Adiabatic Rapid Passage . . . . .	4
<b>3</b>	<b>Chirp</b>	<b>5</b>
<b>4</b>	<b>Scanning Fabry-Pérot Interferometer</b>	<b>7</b>
4.1	Introduction and Motivation . . . . .	7
4.2	Theory . . . . .	7
4.2.1	Resonator losses . . . . .	7
4.2.2	Resonance frequencies, free spectral range and spectral line shapes . . . . .	8
4.2.3	Airy distribution of the Fabry-Pérot interferometer . . . . .	9
4.2.4	Airy linewidth and finesse . . . . .	10
4.2.5	Gaussian Beam . . . . .	12
4.2.6	Higher Gauss Modes . . . . .	14
4.2.7	Mode Matching and Coupling Losses . . . . .	15
4.2.8	Gaussian Beam Focusing . . . . .	17
4.2.9	Confocal Setups . . . . .	18
4.2.10	Simulation . . . . .	18
4.3	Setup . . . . .	18
4.3.1	Flat mirrors . . . . .	18
4.3.2	Concave mirrors . . . . .	18

4.3.3	Confocal setup . . . . .	18
4.4	Measurements and Results . . . . .	18
<b>Bibliography</b>		<b>21</b>

## List of Figures

2.1	Simulated exciton emission of a GaAs quantum dot . . . . .	4
4.1	Fabry-Pérot interferometer with electric field mirror reflectivities $r_1$ and $r_2$ . . . . .	9
4.2	Airy distribution $A'_{trans}$ as described in equation (4.17) compared to the Lorentzian lines $\gamma_{q,L}$ as described in equation (4.14) . . . . .	10
4.3	Demonstration of the physical meaning of the Airy finesse $F_{Airy}$ . . . . .	12
4.4	A Gaussian beam near its beam waist. . . . .	13
4.5	Gaussian modes higher order of a simple Ti-sapphire laser . . . . .	15
4.6	Incident monochromatic beam of light exciting transverse mode $m, n$ of a resonator [7] . . . . .	16
4.7	Spatial filtering of Gauss modes. . . . .	17
4.8	. . . . .	17

# 1 Introduction

Hello, here is some text without a meaning. This text should show what a printed text will look like at this place. If you read this text, you will get no information. Really? Is there no information? Is there a difference between this text and some nonsense like “Huardest gefburn”? Kjift – not at all! A blind text like this gives you information about the selected font, how the letters are written and an impression of the look. This text should contain all letters of the alphabet and it should be written in of the original language. There is no need for special contents, but the length of words should match the language.

This is the second paragraph. Hello, here is some text without a meaning. This text should show what a printed text will look like at this place. If you read this text, you will get no information. Really? Is there no information? Is there a difference between this text and some nonsense like “Huardest gefburn”? Kjift – not at all! A blind text like this gives you information about the selected font, how the letters are written and an impression of the look. This text should contain all letters of the alphabet and it should be written in of the original language. There is no need for special contents, but the length of words should match the language.

And after the second paragraph follows the third paragraph. Hello, here is some text without a meaning. This text should show what a printed text will look like at this place. If you read this text, you will get no information. Really? Is there no information? Is there a difference between this text and some nonsense like “Huardest gefburn”? Kjift – not at all! A blind text like this gives you information about the selected font, how the letters are written and an impression of the look. This text should contain all letters of the alphabet and it should be written in of the original language. There is no need for special contents, but the length of words should match the language.

After this fourth paragraph, we start a new paragraph sequence. Hello, here is some text without a meaning. This text should show what a printed text will look like at this place. If you read this text, you will get no information. Really? Is there no information? Is there a difference between this text and

some nonsense like “Huardest gefburn”? Kjift – not at all! A blind text like this gives you information about the selected font, how the letters are written and an impression of the look. This text should contain all letters of the alphabet and it should be written in of the original language. There is no need for special contents, but the length of words should match the language.

Hello, here is some text without a meaning. This text should show what a printed text will look like at this place. If you read this text, you will get no information. Really? Is there no information? Is there a difference between this text and some nonsense like “Huardest gefburn”? Kjift – not at all! A blind text like this gives you information about the selected font, how the letters are written and an impression of the look. This text should contain all letters of the alphabet and it should be written in of the original language. There is no need for special contents, but the length of words should match the language.

## 2 Quantum Dot

### 2.1 Processing

### 2.2 Properties of our dots

#### 2.2.1 Calculate spectral range of zero-phonon line

A typical lifetime of a GaAs quantum dot is  $\Delta t = 250 \text{ ps}$ . According to the time-energy uncertainty relation

$$\Delta E \cdot \Delta t = \frac{h}{2\pi} \quad (2.1)$$

$$\Rightarrow \Delta E = 2.64 \text{ } \mu\text{eV} \quad (2.2)$$

The frequency uncertainty can be obtained through

$$\Delta \nu = \frac{\Delta E}{h} \quad (2.3)$$

By developing  $\lambda$  into a Taylor series

$$\lambda = \frac{c}{\nu} \quad (2.4)$$

$$\Rightarrow \lambda(\nu) \approx \lambda(\nu_0) + \lambda'(\nu_0) \cdot (\nu - \nu_0) \quad (2.5)$$

$\Delta \lambda$  can be expressed as

$$\Delta \lambda = \lambda(\nu_0 - \Delta \nu) - \lambda(\nu_0) \quad (2.6)$$

$$= \lambda(\nu_0) - \lambda'(\nu_0) \cdot \Delta \nu - \lambda(\nu_0) \quad (2.7)$$

$$= -\lambda'(\nu_0) \cdot \Delta \nu. \quad (2.8)$$

With equation (2.4) this gives

$$\Rightarrow \Delta\lambda = \frac{c}{\nu_0^2} \cdot \Delta\nu = \frac{\lambda_0^2}{c} \cdot \Delta\nu \quad (2.9)$$

$$\approx 1.0 \text{ pm} \quad (2.10)$$

Table 2.1: Parameters of GaAs quantum dots used in the laboratory of semiconductor physics department in Linz. Zero-phonon line calculates from the theoretical limit according to the life time of the excitonic state (as can be seen in equation (??)) up to broader lines which are still valued enough to be measured. The phonon sideband resembles data taken from Schöll et al. [1].

Quantum dot emission	Center wavelength $\lambda_0$	Spectral range $\Delta\lambda$	Waveform
Zero-phonon line	(700 to 800) nm	(1.0 to 1.4) pm	Cauchy
Phonon sideband	0.25 nm higher than zero-phonon line	500 pm	Gauss

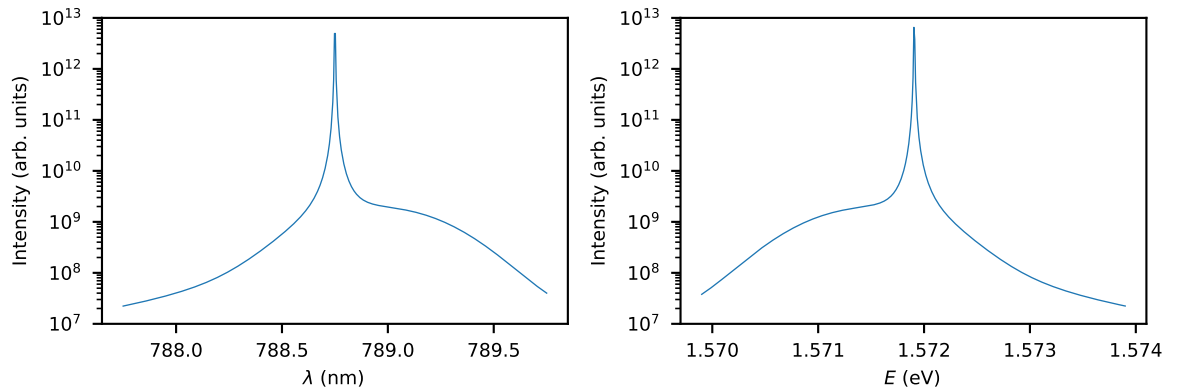


Figure 2.1: Simulated exciton emission of a GaAs quantum dot plotted dependant on the wavelength  $\lambda$  and the Energy  $E$ . The parameters can be found in table 2.1.

Dot-Spectra in far field is ( $\text{TEM}_{00}$ ).

## 2.3 Adiabatic Rapid Passage

## 3 Chirp

Hallo [2]





## 4 Scanning Fabry-Pérot Interferometer

### 4.1 Introduction and Motivation

The Fabry-Pérot interferometer is an optical resonator developed by Charles Fabry and Alfred Pérot. An incoming light beam will only be transmitted through the resonator consisting of two semi-transparent mirrors if it fulfils the resonance condition.[3]

Resolve QD emission line.

### 4.2 Theory

#### 4.2.1 Resonator losses

For the following discussion of the Fabry-Pérot interferometer, a two-mirror-resonator with the reflecting surfaces facing each other and air as medium in between is assumed. The time the light needs for one roundtrip is then given by [4]

$$t_{RT} = \frac{2l}{c} \quad (4.1)$$

where  $l$  is the geometrical length of the resonator and  $c$  is the speed of light in air.

The photon-decay time  $\tau_c$  of the interferometer is then given by

$$\frac{1}{\tau_c} = -\frac{\ln(R_1 \cdot R_2)}{t_{RT}} \quad (4.2)$$

where  $R_1$  and  $R_2$  are the corresponding intensity reflectivities of the mirrors.

The number of photons at frequency  $\nu$  inside the resonator is described by the differential rate equation

$$\frac{d}{dt}\varphi(t) = -\frac{1}{\tau_c}\varphi(t). \quad (4.3)$$

With a number  $\varphi_s$  of photons at  $t = 0$  the integration gives

$$\varphi(t) = \varphi_s e^{-t/\tau_c} \quad (4.4)$$

### 4.2.2 Resonance frequencies, free spectral range and spectral line shapes

The round-trip phase shift at frequency  $\nu$  is given by

$$2\phi(\nu) = 2\pi\nu t_{RT} = 2\pi\nu \frac{2l}{c} \quad (4.5)$$

where  $\phi(\nu)$  is the single-pass phase shift between the mirrors.

Resonances are visible for frequencies  $\nu$  at which the light interferes constructively after one round trip. Two adjacent resonance frequencies differ in their round trip phase shift by  $2\pi$ . Hence, the free spectral range  $\Delta\nu_{FSR}$ , the frequency difference between two adjacent resonance frequencies, can be calculated from equation (4.11)

$$2\Delta\phi_{FSR} = 2\pi \quad (4.6)$$

$$\Rightarrow 2\pi\Delta\nu_{FSR} \frac{2l}{c} = 2\pi \quad (4.7)$$

$$\Rightarrow \Delta\nu_{FSR} = \frac{c}{2l} \quad (4.8)$$

According to equation (4.4) the number of photons decay with the photon-decay time  $\tau_c$ . With  $E_{q,s}$  representing the initial amplitude, the electric field at  $\nu_q$  can be given by

$$E_q(t) = \begin{cases} E_{q,s} e^{i2\pi\nu_q t} e^{-t/(2\tau_c)} & t \geq 0 \\ 0 & t < 0 \end{cases}. \quad (4.9)$$

The Fourier transformation of the electric field can be expressed as

$$\tilde{E}_q(\nu) = \int_{-\infty}^{\infty} E_q(t) e^{-i2\pi\nu t} dt = E_q(t) \int_0^{\infty} e^{[1/(2\tau_c) + i2\pi(\nu - \nu_q)]t} dt = E_{q,s} \frac{1}{(2\tau_c)^{-1} + i2\pi(\nu - \nu_q)}. \quad (4.10)$$

The normalized spectral line shape per unit frequency is then given by

$$\tilde{\gamma}_q(\nu) = \frac{1}{\tau_c} \left| \frac{\tilde{E}_q(\nu)}{E_{q,s}} \right|^2 = \frac{1}{\tau_c} \left| \frac{1}{(2\tau_c)^{-1} + i2\pi(\nu - \nu_q)} \right|^2 = \frac{1}{\tau_c} \frac{1}{(2\tau_c)^{-2} + 4\pi^2(\nu - \nu_q)^2} \quad (4.11)$$

$$= \frac{1}{\pi} \frac{1/(4\pi\tau_c)}{1/(4\pi\tau_c)^2 + (\nu - \nu_q)^2} \quad (4.12)$$

with  $\int \tilde{\gamma}_q(\nu) d\nu = 1$ . By defining the full-width-at-half-maximum linewidth (FWHM)  $\Delta\nu_c$  we get

$$\Delta\nu_c = \frac{1}{2\pi\tau_c} \Rightarrow \tilde{\gamma}_q(\nu) = \frac{1}{\pi} \frac{\Delta\nu_c/2}{(\Delta\nu_c/2)^2 + (\nu - \nu_q)^2} \quad (4.13)$$

By normalizing the Lorentzian lines so that the peak is at unity we finally obtain

$$\gamma_{q,L}(\nu) = \frac{\pi}{2} \Delta\nu_c \tilde{\gamma}_q(\nu) = \frac{(\Delta\nu_c)^2}{(\Delta\nu_c)^2 + 4(\nu - \nu_q)^2} \quad (4.14)$$

with  $\gamma_{q,L}(\nu_q) = 1$ .

### 4.2.3 Airy distribution of the Fabry-Pérot interferometer

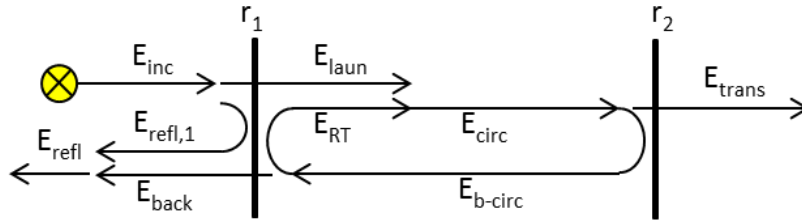


Figure 4.1: Fabry-Pérot interferometer with electric field mirror reflectivities  $r_1$  and  $r_2$ . Indicated in this figure are the electric fields resulting from an incoming  $E_{inc}$ , the reflected field  $E_{refl,1}$  and transmitted field  $E_{laun}$ .  $E_{circ}$  and  $E_{circ,b}$  circulate inside the resonator, resulting in  $E_{RT}$  after one round-trip.  $E_{back}$  is the backwards transmitted field.[5]

The response of the Fabry-Pérot interferometer is calculated with the circulating-field approach [4], where a steady-state is assumed.  $E_{circ}$  is the result of  $E_{laun}$  interfering with  $E_{RT}$ .  $E_{laun}$  is the transmission of the incoming light  $E_{inc}$  and  $E_{RT}$  is  $E_{circ}$  after one round-trip in the resonator, i.e., after the outcoupling losses of mirror 1 and 2. Therefore, the field  $E_{circ}$  can be calculated from  $E_{laun}$  by

$$E_{circ} = E_{laun} + E_{RT} = E_{laun} + r_1 r_2 e^{-i2\phi} E_{circ} \Rightarrow \frac{E_{circ}}{E_{laun}} = \frac{1}{1 - r_1 r_2 e^{-i2\phi}} \quad (4.15)$$

where  $r_1$  and  $r_2$  are the electric-field reflectivities of mirror 1 and 2.

The generic Airy distribution considers only light inside the mirrors and is defined as

$$A_{circ} = \frac{I_{circ}}{I_{laun}} = \frac{|E_{circ}|^2}{|E_{laun}|^2} = \frac{1}{|1 - r_1 r_2 e^{-i2\phi}|^2} = \frac{1}{(1 - \sqrt{R_1 R_2})^2 + 4\sqrt{R_1 R_2} \sin^2(\phi)} \quad (4.16)$$

by using

$$\begin{aligned} |1 - r_1 r_2 e^{-i2\phi}|^2 &= |1 - r_1 r_2 \cos(2\phi) + i r_1 r_2 \sin(2\phi)|^2 = [1 - r_1 r_2 \cos(2\phi)]^2 + r_1^2 r_2^2 \sin^2(2\phi) \\ &= 1 + R_1 R_2 - 2\sqrt{R_1 R_2} \cos(2\phi) = (1 - \sqrt{R_1 R_2})^2 + 4\sqrt{R_1 R_2} \sin^2(\phi) \end{aligned}$$

and additionally  $R_i = r_i^2$  and  $\cos(2\phi) = 1 - 2\sin^2(\phi)$ .

Commonly, light is sent through the Fabry-Pérot resonator. Therefore the following sections will use the Airy distribution  $A'_{trans}$ .

$$A'_{trans} = \frac{I_{trans}}{I_{inc}} = \frac{I_{circ} \cdot (1 - R_2)}{I_{laun} / (1 - R_1)} = (1 - R_1)(1 - R_2) A_{circ} = \frac{(1 - R_1)(1 - R_2)}{(1 - \sqrt{R_1 R_2})^2 + 4\sqrt{R_1 R_2} \sin^2(\phi)} \quad (4.17)$$

$A'_{trans}$  is displayed in figure 4.2 for  $R_1 = R_2$ . The peak value at one of its resonance frequencies calculates as follows

$$A'_{trans} = \frac{(1 - R_1)(1 - R_2)}{(1 - \sqrt{R_1 R_2})^2} \Big|_{R_1=R_2} 1. \quad (4.18)$$

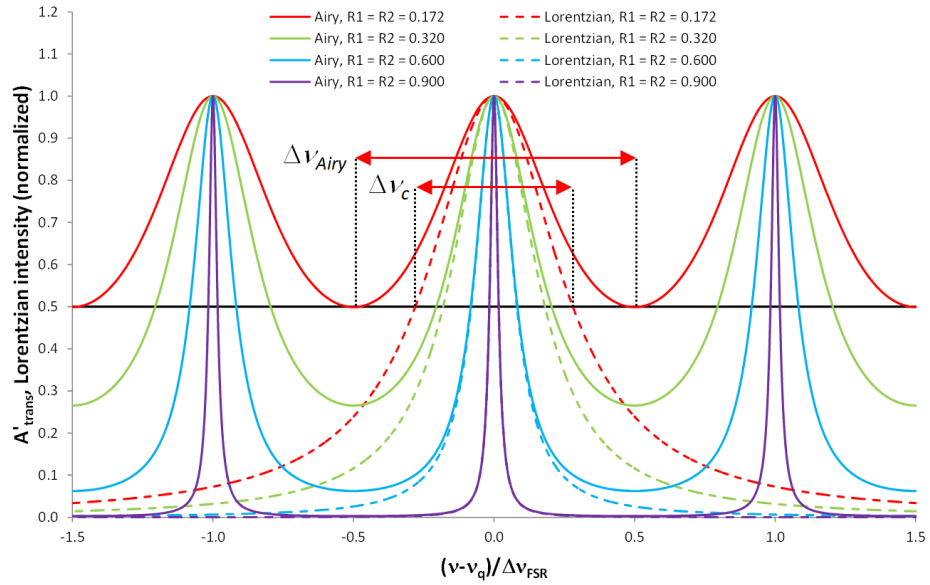


Figure 4.2: Airy distribution  $A'_{trans}$  as described in equation (4.17) compared to the Lorentzian lines  $\gamma_{q,L}$  as described in equation (4.14)

#### 4.2.4 Airy linewidth and finesse

The airy linewidth is defined as the FWHM of  $A'_{trans}$ . It can be set in relation with the free spectral range  $\Delta v_{FSR}$  and the mirror reflectivities as follows.

$A'_{trans}$  decreases to half of its peak value at  $A'_{trans}(v_q)/2$  when the phase shift  $\phi$  changes by the amount

$\Delta\phi$  so that the denominator of  $A'_{trans}$  in equation (4.17) is twice as big

$$\left(1 - \sqrt{R_1 R_2}\right)^2 = 4\sqrt{R_1 R_2} \sin^2(\Delta\phi) \quad (4.19)$$

$$\Rightarrow \Delta\phi = \arcsin\left(\frac{1 - \sqrt{R_1 R_2}}{2\sqrt[4]{R_1 R_2}}\right) \quad (4.20)$$

With equation (4.5) and (4.8), the phase shift can be expressed as

$$\phi = \frac{\pi\nu}{\Delta\nu_{FSR}} \quad (4.21)$$

$$\Rightarrow \Delta\phi = \frac{\pi(\Delta\nu_{Airy}/2)}{\Delta\nu_{FSR}}. \quad (4.22)$$

Therefore, with equation (4.20) and (4.22) the FWHM linewidth is given by

$$\Delta\nu_{Airy} = \Delta\nu_{FSR} \frac{2}{\pi} \arcsin\left(\frac{1 - \sqrt{R_1 R_2}}{2\sqrt[4]{R_1 R_2}}\right). \quad (4.23)$$

The finesse of the Airy distribution of a Fabry-Pérot interferometer is defined as

$$F_{Airy} := \frac{\Delta\nu_{FSR}}{\Delta\nu_{Airy}} = \frac{\pi}{2} \left[ \arcsin\left(\frac{1 - \sqrt{R_1 R_2}}{2\sqrt[4]{R_1 R_2}}\right) \right]^{-1} \quad (4.24)$$

and is therefore only dependent on the mirror reflectivities  $R_1$  and  $R_2$ .

The Airy finesse determining property when it comes to the spectral resolution of the Fabry-Pérot interferometer. This can be made visible by comparing its message with the Taylor criterion for the resolution of two adjacent peaks. The Taylor criterion proposes that two spectral lines are resolvable when the separation of the maxima is greater than the FWHM. As displayed in figure 4.3, the Airy finesse is equal to the number of Airy distributions originating from light at a certain frequencies  $\nu_m$  which do not overlap at a point higher than half of their maxima. Hence, the Airy finesse describes the spectral resolution consistently with the Taylor criterion.

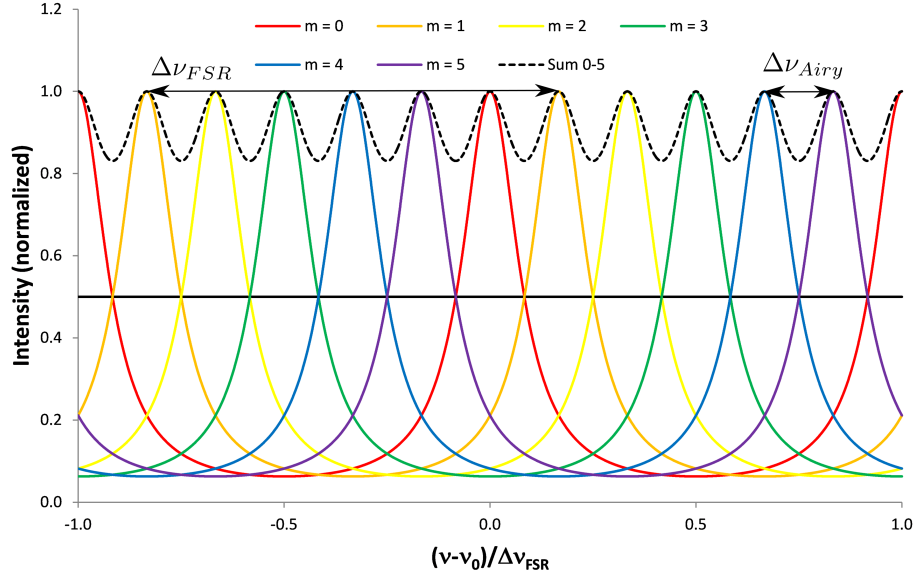


Figure 4.3: Demonstration of the physical meaning of the Airy finesse  $F_{Airy}$ . The coloured lines are Airy distributions created by light at distinct frequencies  $\nu_m$ , while scanning the resonator length. When the light occurs at frequencies  $\nu_m = \nu_q + m\Delta\nu_{Airy}$ , the adjacent Airy distributions are separated from each other by  $\nu_{Airy}$ , therefore fulfilling the Taylor criterion. Since in this example  $F_{Airy} = 6$  exactly six peaks fit inside the free spectral range. As can be seen in the figure the Airy finesse  $F_{Airy}$  quantifies the maximum number of peaks that can be resolved. [5]

#### 4.2.5 Gaussian Beam

In this subsection, light beams are described by the wave picture according to Meschede [6]. They fulfil the Maxwell equations and therefore their electric field  $\mathbf{E}(\mathbf{r}, t)$  the wave equation

$$\left( \nabla^2 - \frac{1}{c^2} \frac{\partial}{\partial t^2} \right) \mathbf{E}(\mathbf{r}, t) = 0. \quad (4.25)$$

Along the propagation direction  $z$  a light beam behaves similarly to a plane wave with constant amplitude  $A_0$  which is a known solution to the wave equation (4.25)

$$E(z, t) = A_0 e^{-i(\omega t - kz)}. \quad (4.26)$$

However, far from its source light is expected to behave like a spherical wave

$$E(\mathbf{r}, t) = A_0 \frac{e^{-i(\omega t - \mathbf{k}\mathbf{r})}}{|\mathbf{r}|}. \quad (4.27)$$

To get a better understanding of the propagation of light, only paraxial (near the  $z$ -axis) parts of the spherical wave are considered. Additionally, the wave is split into its longitudinal ( $z$ -axis) part and it

transversal part and beams with axial symmetry are assumed, which only depend on a transversal coordinate  $\rho$ . Under these circumstances  $\mathbf{kr}$  can be replaced with  $kr$  and because of  $\rho \ll r, z$  the Fresnel approximation can be applied:

$$E(\mathbf{r}) = \frac{A(\mathbf{r})}{|\mathbf{kr}|} e^{i\mathbf{kr}} \simeq \frac{A(z, \rho)}{kz} \exp\left(i \frac{k\rho^2}{2z}\right) e^{ikz} \quad (4.28)$$

with  $r = \sqrt{z^2 + \rho^2} \simeq z + \rho^2/2z$ .

Equation (4.28) resembles the plain wave in equation (4.26), with the spacial phase transversal modulated by  $\exp(ik\rho^2/2z)$ . Another spherical wave solution can be obtained by applying the following replacement ( $z_0$  is a real number)

$$z \rightarrow q(z) = z - iz_0. \quad (4.29)$$

Thereby, the fundamental (or  $\text{TEM}_{00}$ ) Gaussian mode has been constructed

$$E(z, \rho) \simeq \frac{A_0}{kq(z)} \exp\left(i \frac{k\rho^2}{2q(z)}\right) e^{ikz}. \quad (4.30)$$

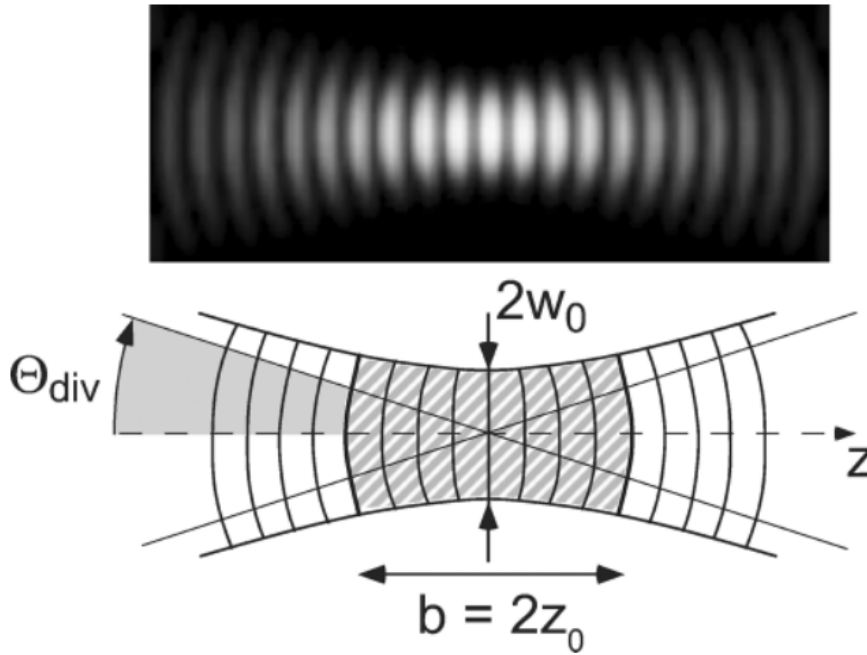


Figure 4.4: A Gaussian beam near its beam waist. Near the center they resemble plan wave fronts, while outside they converge towards spherical wave fronts. The Rayleighzone is shaded at the lower part of the figure.[6]

The electrical and magnetical fields of gauss modes are transversal to its propagation direction. These waveforms are called transversal elctrical and magnetic modes with indices  $(m, n)$ . Its fundamental



solution is the TEM<sub>00</sub>-Mode, which is the most important one and will therefore be examined in more detail in the rest of this subsection.

To express equation (4.30) into a clearer way, the replacement  $q(z) \rightarrow z - iz_0$  will be executed explicitly,

$$\frac{1}{q(z)} = \frac{z + iz_0}{z^2 + z_0^2} = \frac{1}{R(z)} + i \frac{2}{k\omega^2(z)}, \quad (4.31)$$

and new variables  $z_0$ ,  $R(z)$  and  $\omega(z)$  are introduced. With the decomposition of the Fresnel factors into real and imaginary part, two factors can be identified: one complex phase factor, which describes the curvature of the wavefronts and a real factor, which describes the envelope of the beam. Therefore, the exponential in equation (4.30) becomes

$$\exp\left(i \frac{k\rho^2}{2q(z)}\right) \rightarrow \exp\left(i \frac{k\rho^2}{2R(z)}\right) \exp\left(-\left(\frac{\rho}{\omega(z)}\right)^2\right) \quad (4.32)$$

For the following description of gauss modes the following parameters have to be introduced

- **Radius of wavefronts**  $R(z)$ :  $R(z) = z(1 + (z_0/z)^2)$

The greatest curvature or the smallest radius of the wavefronts appear at  $R(z_0) = 2z_0$ .

- **Beam waist**  $2\omega_0$ :  $\omega_0^2 = \lambda z_0 / \pi$

The beam waist  $2\omega_0$  or beam radius  $\omega_0$  describe the smallest beam cross section at  $z = 0$ . If the wave propagates inside a medium with the refractive index  $n$ ,  $\lambda$  has to be replaced with  $\lambda/n$ .

The cross section of the beam waist is then  $\omega_0^2 = \lambda z_0 / (\pi n)$ .

A Gaussian beam can at every point  $z$  on the beam axis be completely characterized either with the parameter couple  $(\omega_0, z_0)$  or alternatively with the real and imaginary part of  $q(z)$ . The parameter of the Gaussian beam are transformed by linear operations, which coefficients are identical to those from geometrical optics:

$$q_{out} = \frac{Aq_{in} + B}{Cq_{in} + D} \quad (4.33)$$

with the parameters  $A, B, C, D$  determined by the optical element transforming the Gaussian beam described by  $q_{in}$ .

#### 4.2.6 Higher Gauss Modes

The wave equation (4.25) can be further simplified, by only allowing monochromatic waves with harmonic time dependence

$$\mathbf{E}(\mathbf{r}, t) = \text{Re} \left( \mathbf{E}(\mathbf{r}) e^{-i\omega t} \right). \quad (4.34)$$

With  $\omega^2 = c^2 \mathbf{k}^2$ , the *Helmholtz equation* can be deduced, which only depends on the location  $\mathbf{r}$

$$(\nabla^2 + k^2) \mathbf{E}(\mathbf{r}) = 0. \quad (4.35)$$

In favour of a formal treatment of the Gaussian modes, the Helmholtz equation is splitted into its transversal and longitudinal contribution,

$$\nabla^2 + k^2 = \frac{\partial^2}{\partial z^2} + \nabla_T^2 + k^2 \quad \text{with} \quad \nabla_T^2 = \frac{\partial}{\partial x^2} + \frac{\partial}{\partial y^2}, \quad (4.36)$$

and apply it on the electric field of equation (4.28). It is assumed that the amplitude  $A$  only changes slowly in the order of the wavelength,

$$\frac{\partial}{\partial z} A = A' \ll kA, \quad (4.37)$$

obtain the approximation

$$\frac{\partial^2}{\partial z^2} A e^{ik\rho^2/(2z)} \frac{e^{ikz}}{kz} \simeq (2ikA' - k^2 A) e^{ik\rho^2/(2z)} \frac{e^{ikz}}{kz}, \quad (4.38)$$

and gain the *paraxial Helmholtz equation*,

$$\left( \nabla_T^2 + 2ik \frac{\partial}{\partial z} \right) A(\rho, z) = 0. \quad (4.39)$$

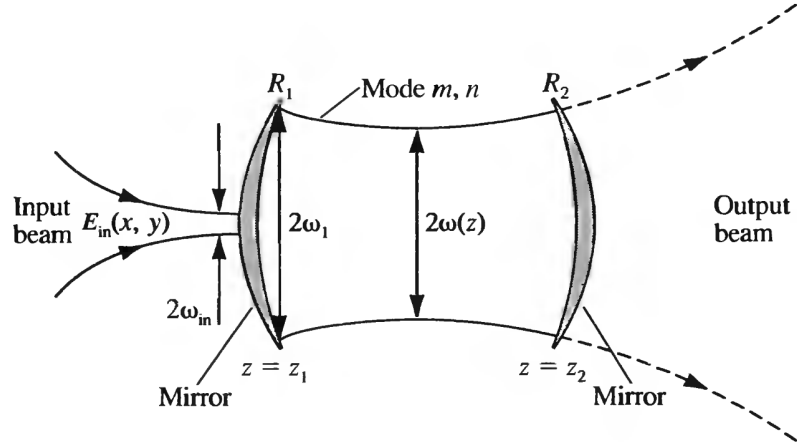
The fundamental solution is the  $\text{TEM}_{00}$  mode in equation (4.30). Examples of higher modes can be found in figure 4.5.



Figure 4.5: Gaussian modes higher order of a simple Ti-sapphire laser. The asymmetry of the high modes are caused by technical inaccuracies of the resonator elements (mirrors, laser crystal).

#### 4.2.7 Mode Matching and Coupling Losses

One basic problem of Fabry P rot interferometry is how to couple efficiently an incident beam of light to a given mode of the resonator. The following discussion is based on the work of Yariv, Yeh, and Yariv [7] and Meschede [6].


 Figure 4.6: Incident monochromatic beam of light exciting transverse mode  $m, n$  of a resonator [7]

In accordance with figure 4.6, an input beam  $E_{in}$  propagates to the resonator and potentially excite its modes  $E_{mn}(x, y)$ , where  $m, n$  are the transverse mode integers of the Gaussian beam of the optical resonator. Since the set  $E_{mn}(x, y)$  describes a complete orthogonal set of wavefunctions they satisfy

$$\iint E_{mn}(x, y) E_{m', n'}^*(x, y) dx dy = 0 \quad \text{unless } m = m' \text{ and } n = n'. \quad (4.40)$$

and

$$E_{in}(x, y) = \sum_{mn} a_{mn} E_{mn}(x, y) \quad (4.41)$$

where  $a_{mn}$  are constants. By multiplying both sides of equation (4.41) with  $E_{mn}^*$ , integrating over the whole  $x$ - $y$ -plane and using equation (4.40), the following expression can be obtained

$$a_{mn} = \frac{\iint E_{in}(x, y) E_{mn}^*(x, y) dx dy}{\iint E_{mn}(x, y) E_{mn}^*(x, y) dx dy} \quad (4.42)$$

The efficiency of coupling an incident field into a spatial mode  $E_{mn}$  is defined as

$$\eta_{mn} = \frac{\text{Power coupled into mode } mn}{\text{Total incident power}} = \frac{\iint |a_{mn} E_{mn}(x, y)|^2 dx dy}{\iint |E_{in}(x, y)|^2 dx dy}. \quad (4.43)$$

By inserting equation (4.42) into equation (4.43) the following expression can be obtained

$$\eta_{mn} = \frac{|\iint E_{in}(x, y) E_{mn}^*(x, y) dx dy|^2}{\iint |E_{in}(x, y)|^2 dx dy \cdot \iint |E_{mn}(x, y)|^2 dx dy}. \quad (4.44)$$

From equation (4.44) can be deduced, that a input beam with the *same* spatial dependency as the mode to be excited

$$E_{in}(x, y) \sim E_{mn}(x, y) \quad (4.45)$$

all of the incident power goes into  $E_{mn}$ , i.e.  $\eta_{mn} = 1$  and all other  $\eta_{m'n'}$  are zero. Usually the fundamental  $TEM_{00}$  mode is desired and equation (4.44) implies that a pure Gaussian beam excites only the fundamental mode and the Fabry P rot interferometer irradiates a pure  $TEM_{00}$  mode as well. In practise, additional measures are necessary such as matching the radius of curvature by gaussian beam focusing (subsection 4.2.8) and *spatial filtering*.

It can be seen in figure 4.5 that the effective area of a mode increases with its order  $(m, n)$ . Figure 4.7 shows one way to suppress higher modes consisting of a focusing lens and a pin hole which diameter  $TEM_{00}$  mode.

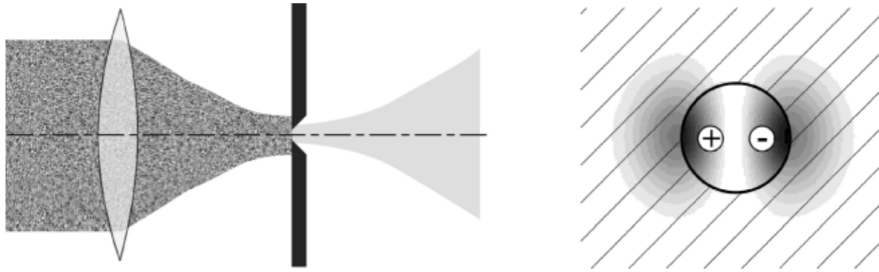


Figure 4.7: Spatial filtering of Gauss modes. In front of the aperture, the beam consists of a superposition of multiple Gauss modes. In the example of  $TEM_{01}$  is displayed, how higher modes are suppressed by the aperture. [6]

#### 4.2.8 Gaussian Beam Focusing

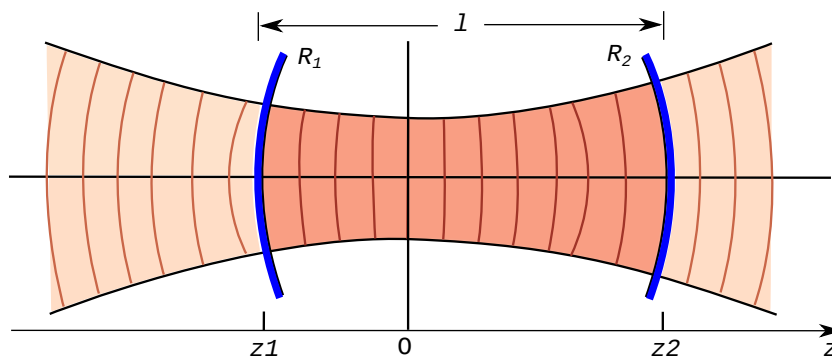


Figure 4.8:

### **4.2.9 Confocal Setups**

#### **4.2.10 Simulation**

## **4.3 Setup**

### **4.3.1 Flat mirrors**

### **4.3.2 Concave mirrors**

### **4.3.3 Confocal setup**

## **4.4 Measurements and Results**

# Appendix



# Bibliography

- [1] Eva Schöll et al. "Resonance fluorescence of GaAs quantum dots with near-unity photon indistinguishability." In: *Nano Letters* 19.4 (Apr. 10, 2019), pp. 2404–2410. ISSN: 1530-6984, 1530-6992. DOI: 10.1021/acs.nanolett.8b05132. arXiv: 1901.09721. URL: <http://arxiv.org/abs/1901.09721> (visited on 05/09/2019) (cit. on p. 4).
- [2] Toshiyuki Hirayama and Mansoor Sheik-Bahae. "Real-time chirp diagnostic for ultrashort laser pulses." In: *Optics Letters* 27.10 (May 15, 2002), p. 860. ISSN: 0146-9592, 1539-4794. DOI: 10.1364/OL.27.000860. URL: <https://www.osapublishing.org/abstract.cfm?URI=ol-27-10-860> (visited on 12/11/2018) (cit. on p. 5).
- [3] Timo Kaldewey et al. "Coherent and robust high-fidelity generation of a biexciton in a quantum dot by rapid adiabatic passage." In: *Physical Review B* 95.16 (Apr. 10, 2017). ISSN: 2469-9950, 2469-9969. DOI: 10.1103/PhysRevB.95.161302. arXiv: 1701.01371. URL: <http://arxiv.org/abs/1701.01371> (visited on 12/11/2018) (cit. on p. 7).
- [4] Nur Ismail et al. "Fabry-Pérot resonator: spectral line shapes, generic and related Airy distributions, linewidths, finesses, and performance at low or frequency-dependent reflectivity." In: *Optics Express* 24.15 (July 25, 2016), p. 16366. ISSN: 1094-4087. DOI: 10.1364/OE.24.016366. URL: <https://www.osapublishing.org/abstract.cfm?URI=oe-24-15-16366> (visited on 02/15/2019) (cit. on pp. 7, 9).
- [5] *Fabry-Pérot interferometer* - Wikipedia. URL: [https://en.wikipedia.org/wiki/Fabry%E2%80%93P%C3%A9rot\\_interferometer](https://en.wikipedia.org/wiki/Fabry%E2%80%93P%C3%A9rot_interferometer) (visited on 05/06/2019) (cit. on pp. 9, 12).
- [6] Dieter Meschede. *Optik, Licht und Laser*. 3., durchges. Aufl. Studium. OCLC: 254422596. Wiesbaden: Vieweg + Teubner, 2008. 568 pp. ISBN: 978-3-8351-0143-2 (cit. on pp. 12, 13, 15, 17).
- [7] Amnon Yariv, Pochi Yeh, and Amnon Yariv. *Photonics: optical electronics in modern communications*. 6th ed. The Oxford series in electrical and computer engineering. OCLC: ocm58648003. New York: Oxford University Press, 2007. 836 pp. ISBN: 978-0-19-517946-0 (cit. on pp. 15, 16).